Structural and Optical Properties of Copper Indium Oxide Nanocrystalline Powders Prepared by Solid-State Reaction Method

Lakshmi Rajesh Ch, Madhusudhana Rao N.*

Department of Physics, School of Advanced Sciences, VIT-AP University, 522237 Andhra Pradesh, India

Copper Indium Oxide ($CuInO_2$) nanocrystalline powder samples with different Cu/In ratios were prepared using the conventional solid-state reaction method. The structural, morphological, and optical properties of $CuInO_2$ samples were studied. The delafossite structure of copper indium oxide nanocrystalline samples with (0 1 2) preferential orientation is observed. With altering the composition, the particles size of the prepared powder samples changed ranging from 6 nm to 94 nm, and the energy band gaps varied from 2.20 eV to 2.37 eV. Photoluminescence intensity at 595 nm and 596 nm in the visible region enhanced with variation of Cu/In ratios.

Keywords: Copper indium oxide, Solid-state reaction, Nanocrystalline powder, Photoluminescence.

1. INTRODUCTION

In recent days, transparent conducting oxides (TCOs) play an important role in our daily life with emerging new technologies. Copper indium oxide (CIO) finds potential applications in the area of flat panel displays, photovoltaic cells [1], passive electrodes, gas sensors, optoelectronic devices, and *p-n* junction devices [2]. The basic TCOs are SnO_2, In_2O_3, ZnO and CdO [3] in the electronic industry. After the advancement of materials implemented *n*-type and *p*-type TCOs, *n*-type TCOs have limited applications compared to *p*-type TCOs [2]. In recent years, *p*-type transparent conducting oxides AMO_2 have been developed with delafossite structure [4, 5], where A is a univalent metal like Ag^+, Cu^+, Pd^+, and Pt^+; M is a trivalent metal group like Al [6], In [2], Ga [7], Nd [8]. CIO with delafossite structure is useful for homogeneous structural *p-n* junctions [2, 8, 9] because it exhibits both *n*-type and *p*-type conductivity with proper dopants like Sn, Ca, Mg, N, and K. Solid-state reaction [5], cation exchange reaction [10] and film preparations through pulsed laser deposition [2], reactive evaporation [11] and RF magnetron sputtering [3] methods are employed to prepare the CIO compound. $CuInO_2$, $Cu_2In_2O_5$, and $CuIn_2O_4$ are the three different copper indium oxides that may form through the solid-state reaction method. Since noble metal oxides are employed as reagents, they typically decompose before the reaction process. Oxides with noble metals are difficult to manufacture using a traditional solid-state reaction. Ponmudi et al. mentioned that mixed metal oxides have received a lot of attention recently because the combined properties of the combined metal oxides make the prepared materials potentially useful. It should be noted that charge redistribution, new electronic states, charge transfer between valence bands, and semiconducting oxide conduction occurred within a mixed metal oxide system, resulting in a variation in energy bandgap in the prepared samples [12, 13]. CIO nanocrystalline powder preparation was complicated via a general solid-state reaction process due to metal oxides easily decomposing and forming either $CuInO_2$ or $Cu_2In_2O_5$. The present work is carried out with the aim of obtaining copper indium oxide nanocrystalline powder via general solid-state reaction in ambient atmosphere with different compositions.

2. EXPERIMENTAL DETAILS

Pure Cu_2O (99.99 %, Sigma Aldrich) and In_2O_3 (99.99 %, Sigma Aldrich) powders were taken in different ratios like 50:50, 60:40, and 40:60 as source material. Using mortar and pestle, powder samples were mixed thoroughly for 16 h of grinding. Prepared samples were kept in quartz glass tubes and placed in a programmable furnace. Samples were sintered in air at 1000 °C and maintained the proper reaction time with a 5 °C/min to 10 °C/min heating/cooling rate. The final product of the copper indium oxide powder appeared in green color. The samples were named as S-I (50 %:50 %), S-II (60 %:40 %), and S-III (40 %:60 %). Once again, the samples were thoroughly ground before the characterization of the samples for structural, optical and morphological studies.

The prepared powder samples were characterized using an X-ray diffractometer (D8 Advance, BRUKER), to study the structural aspects. Morphological study was carried using FESEM (Oxford make Inca Penta FETX3 EDS attachment in carl Zeiss EVO MA 15 SEM instrument). Diffused reflectance of the same was recorded using a UV-VIS-NIR spectrophotometer (JASCO-V-670) in the range of 200 to 2500 nm, and photoluminescence spectra were taken on a HORIBA FL-1000 spectrophotometer in the emission mode.

3. RESULTS AND DISCUSSION

3.1 Structural Properties

Fig. 1 depicts the X-ray diffraction patterns of copper indium oxide nanocrystalline powder samples prepared with different compositions. The XRD patterns confirm the formation of copper indium oxide $CuInO_2$

---

* drnmrao@gmail.com

phase with orientation of the planes (0 0 6), (0 1 2), (1 1 9), (0 1 5), (0 0 9), (1 1 0), (1 0 10), (0 0 12) and (1 0 11) and good crystallinity. All the diffraction peaks matched with the data reported in the literature for copper indium oxide (JCPDS file No: 53-0954), forming delafossite rhombohedral structure. All the observed peaks mapped to the $CuInO_2$ delafossite structure [5, 6]. A major peak was observed in all samples S-I, S-II, and S-III at 33.212°, 33.163°, and 33.017°, respectively, but for the corresponding $CuInO_2$ XRD peak is at 32.96°. A similar small deviation in 2θ was reported by Mandeep Singh et al. [3], by means of X-ray diffraction at the glancing angle, the main peak at 33° was observed for one sample. Charles W. Teplin et al. observed a strong peak at 33.10°, which corresponds to $CuInO_2$ (JCPDS file No 53-0954). Bindhu G. Nair et al. [14] observed the XRD peak at 33.03° for copper indium oxide film of the pure sample prepared through oxygen plasma enhanced reactive evaporation method.
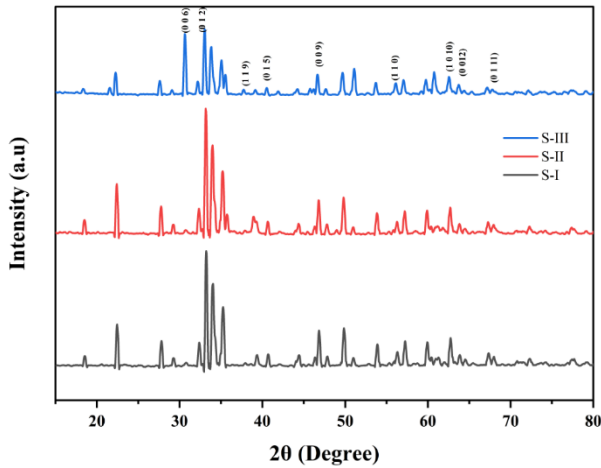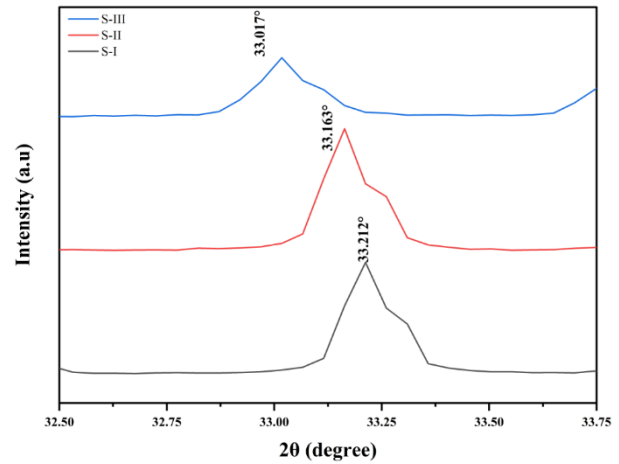

Fig. 1 – X-ray diffraction patterns of the copper indium oxide nanocrystalline powder samples S-I (50:50), S-II (60:40), and S-III (40:60) compositions of $Cu_2O:In_2O_3$

When comparing the three samples of XRD peaks data, sample-III matches with the JCPDS of $CuInO_2$ than the other two samples. And $Cu_2In_2O_5$ (JCPDS file No 30-0479) form is observed in the prepared samples by few peaks nearly at 22.26°, 33.74°, 35.15°, 49.66°, 57.10°, and 59.73°. Ginley et al. [1] stated that the deposition of materials above 600 °C results in XRD peaks indicating a mixture of $CuInO_2$ and In_2O_3. The variation of XRD results of copper indium oxide presented in Fig. 2 shows some deviations in the prepared powder samples of 2θ peak values compared to 2θ of XRD peaks of $CuInO_2$ prepared through cation exchange reaction [5]. The formula for finding the lattice parameters of copper indium oxide with delafossite rhombohedral structure [5] with the hexagonal crystal lattice is

$$\frac{1}{d^2} = \frac{4}{3}\left(\frac{h^2 + hk + k^2}{a^2}\right) + \frac{l^2}{c^2}, \tag{1}$$

where d is the inter-planar spacing of the crystal planes, hkl are the Miller indices and a and c are the lattice parameters of the crystal system. The XRD peaks of the prepared samples S-I, S-II, and S-III at respective 2θ values confirmed the formation of a

rhombohedral structure with the lattice parameters $a = 3.269$ Å and $c = 17.49$ Å which are very similar to the delafossite $CuInO_2$ (JCPDS file No 53-0954) $a = 3.292$ Å and $c = 17.388$ Å.

Fig. 2 – The enlarged view of the X-ray diffraction pattern of copper indium oxide nanocrystalline powder samples S-I, S-II, and S-III in the diffraction angle range of 32.5° to 33.75°

A summary of the ratio of Cu/In, crystallite size, and the bandgap of prepared samples at a temperature of 1000 °C of copper indium oxide nanocrystalline powder samples is given in Table 1. From XRD data, using the Debye-Scherrer formula, the average crystallite size of the prepared powder samples of copper indium oxide was calculated and listed in the table.

The X-ray diffraction method trusts on this broadening of diffraction peaks, which occurs when tiny crystallites cause atoms in crystal unit cells to be shifted from their optimum position (size broadening) less than one micrometer in size and an abundance of crystal lattice defects (strain broadening) such as dislocations [15]. The dislocation density (δ) was calculated for the prepared samples from the following relation [16]:

$$\delta = \frac{1}{D^2}, \tag{2}$$

where D is the mean crystallite size in nm. Sofi et al. [17] observed the doping concentration grew from 0 to 7 %, and dislocation density values of a declining trend order indicated a shift in disorder in Cu doped In_2O_3 through the citrate gel process. And through the solid-state reaction process also observed an increase in dislocation density in the prepared indium-rich samples and a decrease in the dislocation density in the copper-rich sample.

3.2 Morphological Studies

Fig. 3a shows the particle diameter from 15 to 94 nm, Fig. 3b reveals the particle diameter in the range of 6 to 95 nm, and Fig. 3c shows the particle diameter in the range of 7 to 88 nm. Fig. 3d shows that the average particle size is seen to increase from nano to a few micros with varying the composition of Cu_2O and In_2O_3. The size of the agglomeration in samples that have been observed is not uniform. The observed grain sizes in FESEM are nearly equal to those calculated from the XRD data.

Table 1 – Summary of the ratio of Cu/In, crystallite size, and bandgap of prepared samples at a temperature of 1000 °C

Sample name	Ratio of Cu/In	2θ (degree)	FWHM β (°)	Crystallite size (nm), XRD	Dislocation density (δ) 10^{15} m^{-2}	Bandgap (eV)
S-I	50:50	33.212	0.2991	27.71	1.30	2.28
S-II	60:40	33.163	0.2993	27.69	1.304	2.20
S-III	40:60	33.017	0.3025	27.38	1.333	2.37
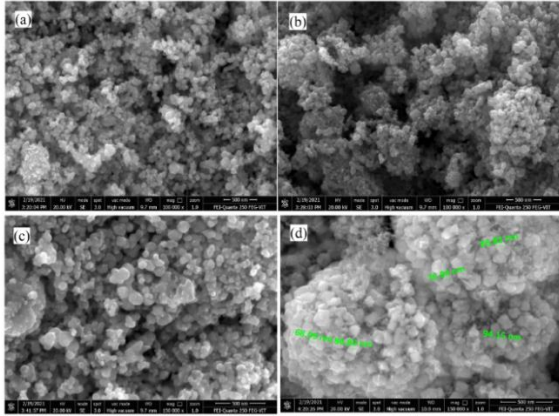
Fig. 3 – FESEM images of copper indium oxide: (a) S-I (50:50), (b) S-II (60:40), (c) S-III (40:60) nanocrystalline powder samples, and (d) enlarged view of sample S-III

Fig. 4 – Optical reflectance spectra of copper indium oxide nanocrystalline powder samples: S-I (50:50), S-II (60:40), and S-III (40:60) with the compositions of $Cu_2O:In_2O_3$

3.3 Optical Properties

The optical properties of the prepared copper indium oxide powder samples were studied by using diffuse reflectance spectra in the UV-Vis region. Fig. 4 shows the diffuse reflectance spectra recorded at room temperature in the wavelength range 200-1100 nm. From these spectra, it may be observed as a decreasing trend when the concentration of In_2O_3 increased in the samples. The bandgap of copper indium oxide powder samples with various compositions of copper and indium at a temperature of 1000 °C can be calculated by the Kubelka-Munk function:
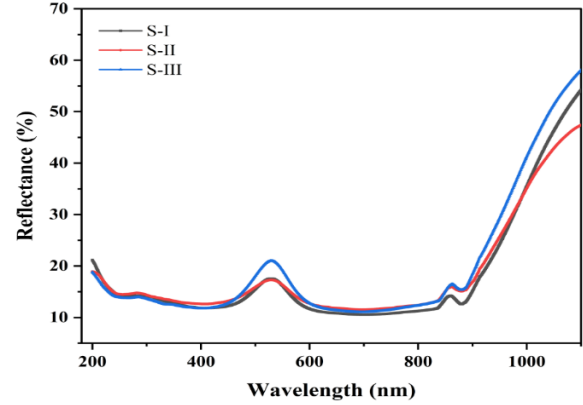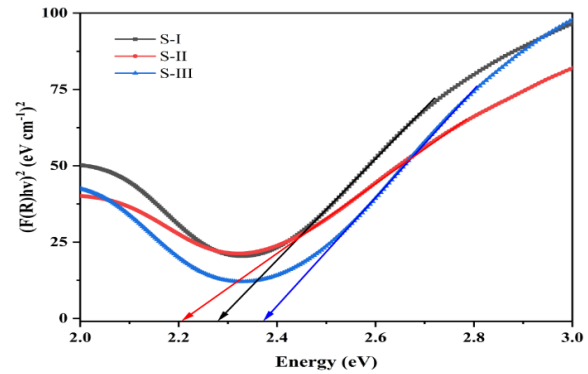
$$F(R) = \frac{\left(1 - R^2\right)}{2R} = \frac{\alpha}{S}, \qquad (3)$$

where $F(R)$ is the Kubelka-Munk function, R is the diffuse reflectance, α is the absorption coefficient, and S is the scattering coefficient [18].

Fig. 5 shows the optical energy bandgaps of copper indium oxide powder samples with different compositions of $Cu_2O:In_2O_3$. The value was obtained by plotting $(F(R)h\nu)^2$ vs photon energy ($h\nu$), after extrapolating the linear region ($F(R) = 0$). The optical band gap was calculated by plotting Tauc plots with the Kubelka-Munk function using the below relation:

$$\left[F(R)h\nu\right]^2 = A\left(h\nu - E_g\right), \qquad (4)$$

where h, ν, A, and E_g are the Plank constant, light frequency, proportionality constant, and energy band gap of the sample, respectively [19]. By using Eq. (4), the energy bandgaps of the prepared copper indium oxide powder samples S-I (50:50), S-II (60:40) and S-III (40:60) were observed equal to 2.28, 2.20 and 2.37 eV.

Fig. 5 – Plot of $(F(R)h\nu)^2$ vs energy ($h\nu$) of copper indium oxide nanocrystalline powder samples at S-I (50:50), S-II (60:40), and S-III (40:60)

3.4 Photoluminescence Studies

Non-destructive photoluminescence (PL) was used to investigate inherent and extrinsic defects in semiconductors. This approach, which is based on concentration, offers information regarding impurity and defective energy states. Understanding defect structures is important in semiconductors. PL spectra of the copper indium oxide nanocrystalline powder samples S-I, S-II, and S-III were recorded at room temperature with an excitation wavelength of 540 nm, as shown in Fig. 6.

The absorption of photons creates electron-hole pairs when the material is stimulated with a specific wavelength. The recombination of electron and hole pairs in nanoparticles causes the band edge emission. From the PL spectra, all the samples show emission bands ranging from 585 to 825 nm. Sample S-I with $Cu_2O:In_2O_3$ (50:50) showed a strong PL peak at 595 nm and a weak peak at 788 nm. S-II containing $Cu_2O:In_2O_3$ (60:40) showed a strong peak at 595 nm.
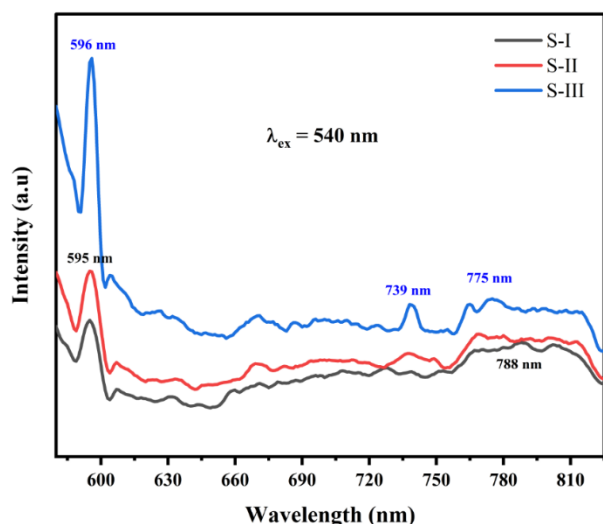
Fig. 6 – PL spectra of copper indium oxide powder samples S-I (50:50), S-II (60:40), and S-III (40:60)

Also, S-III containing $Cu_2O:In_2O_3$ (40:60) showed a strong peak at 596 nm and two weak peaks observed at 739 nm and 775 nm. We can say that the PL in copper indium oxide is due to the presence of traces of either Cu_2O or In_2O_3. Pinki Devi et. al [20] observed that a peak at 781 nm is formed in the samples due to an oxygen vacancy defect. Sergio Roso et al. [21] produced

In_2O_3 octahedra using a vapor-phase transport technique and detected a PL strong emission peak at 600 nm. This suggests the presence of an orange emission band thought to originate in nanomaterials deep indium interstitials.

4. CONCLUSIONS

Copper indium oxide nanocrystalline powders were prepared by solid-state reaction with different compositions at 1000 °C using Cu_2O and In_2O_3. The prepared powder samples had a green color with good crystallinity, the average crystallite size was nearly 20.20, 22.31, and 30.57 nm. The particles of the powder samples were in the nanoscale range from 6 to 94 nm and have an energy band gap of 2.20 to 2.37 eV. Copper indium oxide shows strong emission peaks at 595 and 596 nm in the PL spectra for the variation of Cu_2O and In_2O_3 ratios.

REFERENCES

1. D. Ginley, B. Roy, A. Ode, C. Warmsingh, Y. Yoshida, P. Parilla, C. Teplin, T. Kaydanovaa, A. Miedanera, C. Curtisa, A. Martinson, T. Coutts, D. Readey, H. Hosono, J. Perkins, *Thin Solid Films* **445**, 193 (2003).
2. H. Yanagi, T. Hase, S. Ibuki, K. Ueda, H. Hosono, *Appl. Phys. Lett.* **78**, 1583 (2001).
3. M. Singh, V.N. Singh, B.R. Mehta, *J. Nanosci. Nanotechnol.* **8**, 3889 (2008).
4. C.W. Teplin, T. Kaydanova, D.L. Young, J.D. Perkins, David S. Ginley, *Appl. Phys. Lett.* **85**, 3789 (2004).
5. M. Shimode, M. Sasaki, K. Mukaida, *J. Solid State Chem.* **151**, 16 (2000).
6. H. Yanagi, Shin-ichiro Inoue, K. Ueda, H. Kawazoe, H. Hosono, N. Hamada, *J. Appl. Phys.* **88**, 4159 (2000).
7. K. Ueda, T. Hase, H. Yanagi, H. Kawazoe, H. Hosono, *J. Appl. Phys.* **89**, 1790 (2001).
8. K. Nomura, H. Ohta, K. Ueda, T. Kamiya, M. Orita, M. Hirano, *J. Appl. Phys.* **95**, 5532 (2004).
9. J-C. Lee, Y-W. Heo, J-H. Lee, J-J. Kim, *Thin Solid Films* **518**, 1234 (2009).
10. W. Gessner, *Silikattechnik* **21**, 45 (1970).
11. S.A. Mary, B.G. Nair, J. Naduvath, G.S. Okram, S.K. Remillard, P.V. Sreenivasan, R.R. Philip, *J. Alloy. Compd.* **600**, 159 (2014).
12. S. Ponmudi, R. Sivakumar, C. Sanjeeviraja, C. Gopalakrishnan, *J. Mater. Sci.: Mater. Electron.* **30**, 18315 (2019).
13. E.M. Alkoy, P.J. Kelly, *Vacuum* **79**, 221 (2005).
14. Bindu G. Nair, Julie Ann Joseph, Z.T. Kellner, Vikash Sharma, S.K. Remillard, P.A. DeYoung, G.S. Okram, V. Ganesan, Rachel Reena Philip, *J. Alloy. Compd.* **746**, 435 (2018).
15. T. Ungar, *Scripta Mater.* **51**, 777 (2004).
16. H. Siddiqui, M.S. Qureshi, F.Z. Haque, *Optik* **125** No 17, 4663 (2014).
17. A.H. Sofi, M.A. Shah, *Mater. Res. Exp.* **6**, 045039 (2019).
18. Džimbeg-Malčić, Ž. Barbarić-Mikočević, K. Itrić, Teh. Vjesn. Znan. Časopis Teh. Fak. Sveučilišta u Osijeku. **18**, 117 (2011).
19. S.S. Abdullahi, S. Güner, Y. Koseoglu, I.M. Musa, B.I. Adamu, M.I. Abdulhamid, *J. NAMP* **35**, 241 (2016).
20. Pinki Devi, Arunima Singh, Karan Malik, Anil Verma, Saswata Bhattacharya, Jitendra Pratap Singh, *J. Electrochem. Soc.* **168**, 066518 (2021).
21. Sergio Roso, Carla Bittencourt, Polona Umek, Oriol González, Frank Güell, Atsushi Urakawa, Eduard Llobet, *J. Mater. Chem. C* **4**, 9418 (2016).

Структурні та оптичні властивості нанокристалічних порошків оксиду міді індію, отриманих методом твердофазної реакції

Lakshmi Rajesh Ch, Madhusudhana Rao N

Department of Physics, School of Advanced Sciences, VIT-AP University, 522237 Andhra Pradesh, India

Зразки нанокристалічного порошку оксиду міді індію ($CuInO_2$) з різними співвідношеннями Cu/In були виготовлені за допомогою звичайного методу твердофазної реакції. Досліджено структурні, морфологічні та оптичні властивості зразків $CuInO_2$. Спостерігається делафоситна структура нанокристалічних зразків оксиду міді індію з переважною орієнтацією (012). Зі зміною складу розмір частинок виготовлених порошкових зразків змінювався в межах від 6 до 94 нм, а ширина забороненої зони варіювалася від 2,20 до 2,37 еВ. Інтенсивність фотолюмінесценції при 595 і 596 нм у видимій області підсилювалася зі зміною співвідношення Cu/In.

Ключові слова: Оксид міді індію, Твердотільна реакція, Нанокристалічний порошок, Фотолюмінесценція.